Transitions between the 4f-core-excited states in Ir^{16+},Ir^{17+}, and Ir^{18+} ions for clock applications

U. I. Safronova, V. V. Flambaum, and M. S. Safronova

Phys. Rev. A **92**, 022501 — Published 5 August 2015

DOI: 10.1103/PhysRevA.92.022501

Transitions between the $4f$-core-excited states in Ir^{16+}, Ir^{17+}, and Ir^{18+} ions for clock applications

U. I. Safronova
Physics Department, University of Nevada, Reno, Nevada 89557

V. V. Flambaum
University of New South Wales, Sydney 2052, Australia

M. S. Safronova
Department of Physics and Astronomy, University of Delaware, Newark, Delaware 19716 and Joint Quantum Institute, NIST and the University of Maryland, College Park, Maryland 20899, USA

Iridium ions near $4f$-$5s$ level crossings are the leading candidates for a new type of atomic clocks with a high projected accuracy and a very high sensitivity to the temporal variation of the fine structure constant α. To identify spectra of these ions in experiment accurate calculations of the spectra and electromagnetic transition probabilities should be performed. Properties of the $4f$-core-excited states in Ir^{16+}, Ir^{17+}, and Ir^{18+} ions are evaluated using relativistic many-body perturbation theory and Hartree-Fock-Relativistic method (COWAN code). We evaluate excitation energies, wavelengths, oscillator strengths, and transition rates. Our large-scale calculations included the following set of configurations: $4f^{14}5s$, $4f^{14}5p$, $4f^{13}5s^2$, $4f^{13}5p^2$, $4f^{13}5s5p$, $4f^{12}5s^25p$, and $4f^{12}5s5p^2$ in Pm-like Ir^{16+} ; $4f^{14}$, $4f^{13}5s$, $4f^{13}5p$, $4f^{12}5s^2$, $4f^{12}5s5p$, and $4f^{12}5p^2$ in Nd-like Ir^{17+}; and $4f^{13}$, $4f^{12}5s$, $4f^{12}5p$, $4f^{11}5s^2$, and $4f^{11}5s5p$ in Pr-like Ir^{18+}.

The $5s-5p$ transitions are illustrated by the synthetic spectra in the 180 - 200 Å range. Large contributions of magnetic-dipole transitions to lifetimes of low-lying states in the region below 2.5 Ry are demonstrated.

PACS numbers: 31.15.ag, 31.15.aj, 31.15.am, 31.15.vj

I. INTRODUCTION

Selected transitions involving electron holes, i.e. vacancies in otherwise filled shells of atomic systems in highly-charged ions were shown to have frequencies within the range of optical atomic clocks, have small systematic errors in the frequency measurements and be highly sensitive to the temporal variation of the fine structure constant α [1]. Sympathetic cooling of highly-charged ions has been demonstrated in [2].

This work is motivated by these applications of highly-charged ions and recent experimental work including identification of M1 transitions in Ir^{17+} spectra [2–4]. In 2015, identification of the predicted $5s-4f$ level crossing optical transitions was presented by Windberger *et al.* [3]. The spectra of Nd-like W, Re, Os, Ir, and Pt ions of particular interest for tests of fine-structure constant variation were explored [3]. The authors exploited characteristic energy scalings to identify the strongest lines, confirmed the predicted $5s-4f$ level crossing, and benchmarked advanced calculations.

In the present work, we have employed Hartree-Fock-Relativistic method (COWAN code) and relativistic many-body perturbation theory (RMBPT) to study Ir^{16+}, Ir^{17+}, and Ir^{18+} ions. Excitation energies, wavelengths, transition rates, energies of the lower and upper level, lifetimes, and branching ratios from M1 and E1 transitions in Nd-, Pm-, and Pr-like Ir ions are evaluated. The scaling of electrostatic integrals in the Cowan code allows us to correct for correlation effects and to obtain good agreement with experimental energies. We employed a single scaling factor (0.85) for all electrostatic integrals. We have used our results to construct synthetic spectra for all three ions. Our goal was to also to investigate the general structure and level distributions in these ions. For example, we find that in the case of Ir^{18+} ion, the energies of the $4f^{13}$, $4f^{12}5s$, and

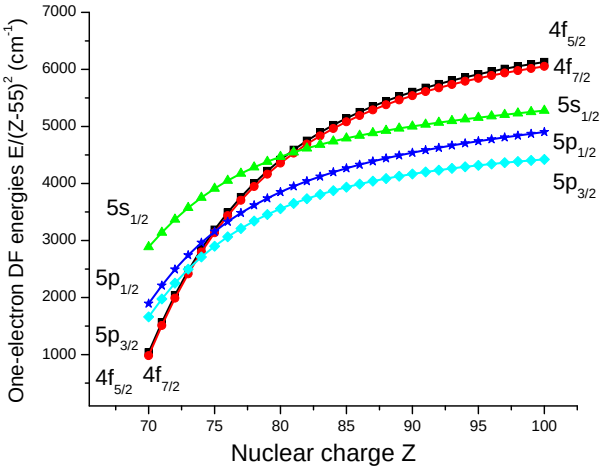

FIG. 1: Dirac-Fock binding energies of the $4f$, $5s$, and $5p$ orbitals as a function of Z in Er-like ions. Er is a rare earth element with $Z = 68$.

TABLE I: Energies (in cm^{-1}) in Pm-like Ir^{16+}, Nd-like Ir^{17+}, and Pr-like Ir^{18+} ions given relative to the $4f^{13}5s^2\ {}^2F_{7/2}$, $4f^{13}5s\ {}^3F_4$, and $4f^{13}\ {}^2F_{7/2}$ ground states, respectively.

Conf.	Level	Energy	Conf.	Level	Energy	Conf.	Level	Energy
	Pm-like Ir^{16+} ion			Nd-like Ir^{17+} ion			Pr-like Ir^{18+} ion	
$4f^{13}5s^2$	$(^2F)^2F_{7/2}$	0	$4f^{13}5s$	$(^2F)^3F_4$	0	$4f^{13}$	$(^2F)^2F_{7/2}$	0
$4f^{13}5s^2$	$(^2F)^2F_{5/2}$	25909	$4f^{13}5s$	$(^2F)^3F_3$	4236	$4f^{13}$	$(^2F)^2F_{5/2}$	26442
$4f^{14}5s$	$(^1S)^2S_{1/2}$	28350	$4f^{14}$	$(^1S)^1S_0$	5091	$4f^{12}5s$	$(^3H)^4H_{13/2}$	60142
$4f^{13}5s5p$	$(^2F)^4D_{7/2}$	267942	$4f^{13}5s$	$(^2F)^3F_2$	26174	$4f^{12}5s$	$(^3H)^4H_{11/2}$	67687
$4f^{12}5s^25p$	$(^3H)^4G_{11/2}$	276214	$4f^{13}5s$	$(^2F)^1F_3$	30606	$4f^{12}5s$	$(^3F)^4F_{9/2}$	70096
$4f^{12}5s^25p$	$(^3H)^2I_{13/2}$	280511	$4f^{12}5s^2$	$(^3H)^3H_6$	33856	$4f^{12}5s$	$(^1G)^2G_{7/2}$	74664
$4f^{12}5s^25p$	$(^3F)^4D_{7/2}$	285301	$4f^{12}5s^2$	$(^3F)^3F_4$	42199	$4f^{12}5s$	$(^3H)^4H_{9/2}$	87749
$4f^{13}5s5p$	$(^2F)^4D_{7/2}$	286286	$4f^{12}5s^2$	$(^3H)^3H_5$	58261	$4f^{12}5s$	$(^3H)^2H_{11/2}$	89859
$4f^{12}5s^25p$	$(^1G)^2H_{9/2}$	287909	$4f^{12}5s^2$	$(^3F)^3F_2$	63696	$4f^{12}5s$	$(^3F)^4F_{3/2}$	92406
$4f^{13}5s5p$	$(^2F)^4G_{9/2}$	288623	$4f^{12}5s^2$	$(^3H)^3H_4$	66296	$4f^{12}5s$	$(^3F)^4F_{5/2}$	92940
$4f^{13}5s5p$	$(^2F)^4F_{5/2}$	289959	$4f^{12}5s^2$	$(^3F)^3F_3$	68886	$4f^{12}5s$	$(^3F)^4F_{7/2}$	94508
$4f^{13}5s5p$	$(^2F)^4G_{5/2}$	297128	$4f^{12}5s^2$	$(^3H)^3H_4$	89455	$4f^{12}5s$	$(^1G)^2G_{9/2}$	98486
$4f^{12}5s^25p$	$(^3H)^4I_{11/2}$	303063	$4f^{12}5s^2$	$(^3P)^3P_2$	91765	$4f^{12}5s$	$(^3F)^2F_{7/2}$	101805
$4f^{12}5s^25p$	$(^3H)^4G_{9/2}$	303664	$4f^{12}5s^2$	$(^3P)^3P_0$	101073	$4f^{12}5s$	$(^3F)^2F_{5/2}$	102646
$4f^{12}5s^25p$	$(^1D)^2D_{3/2}$	307339	$4f^{12}5s^2$	$(^1I)^1I_6$	101537	$4f^{12}5s$	$(^1G)^2G_{7/2}$	119089
$4f^{12}5s^25p$	$(^3F)^4G_{5/2}$	307948	$4f^{12}5s^2$	$(^3P)^3P_1$	107843	$4f^{12}5s$	$(^3P)^4P_{5/2}$	122306
$4f^{12}5s^25p$	$(^3F)^4G_{7/2}$	309803	$4f^{12}5s^2$	$(^1D)^1D_2$	117322	$4f^{12}5s$	$(^3H)^2H_{9/2}$	123040
$4f^{12}5s^25p$	$(^3H)^4I_{9/2}$	312724	$4f^{12}5s^2$	$(^1S)^1S_0$	178055	$4f^{12}5s$	$(^3F)^4F_{3/2}$	123434
$4f^{12}5s^25p$	$(^3F)^4F_{5/2}$	313871	$4f^{12}5s5p$	$(^3H)^5G_6$	312027	$4f^{12}5s$	$(^3P)^4P_{1/2}$	129563
$4f^{13}5s5p$	$(^2F)^2D^a_{5/2}$	315471	$4f^{13}5p$	$(^2F)^3D_3$	319802	$4f^{12}5s$	$(^1I)^2I_{13/2}$	132511
$4f^{13}5s5p$	$(^2F)^2G^a_{7/2}$	317004	$4f^{12}5s5p$	$(^3F)^5D_4$	321722	$4f^{12}5s$	$(^1I)^2I_{11/2}$	132716
$4f^{12}5s^25p$	$(^3F)^4G_{7/2}$	317387	$4f^{13}5p$	$(^2F)^3G_4$	322623	$4f^{12}5s$	$(^3P)^4P_{3/2}$	136659
$4f^{13}5s5p$	$(^2F)^4F_{3/2}$	319123	$4f^{12}5s5p$	$(^3H)^3I^b_7$	333465	$4f^{12}5s$	$(^3P)^2P_{1/2}$	145476
$4f^{12}5s^25p$	$(^3H)^4I_{9/2}$	332682	$4f^{12}5s5p$	$(^3H)^5G_5$	333531	$4f^{12}5s$	$(^1D)^2D_{5/2}$	147492
$4f^{12}5s^25p$	$(^3P)^4P_{3/2}$	335326	$4f^{12}5s5p$	$(^3H)^5G_6$	333649	$4f^{12}5s$	$(^3P)^2P_{3/2}$	152098
$4f^{12}5s^25p$	$(^3F)^4G_{5/2}$	337196	$4f^{12}5s5p$	$(^3H)^5I_5$	340286	$4f^{11}5s^2$	$(^4I)^4I_{15/2}$	179577
$4f^{14}5p$	$(^1S)^2P_{1/2}$	337757	$4f^{12}5s5p$	$(^1G)^3H_4$	342157	$4f^{11}5s^2$	$(^4F)^4F_{9/2}$	201648

$4f^{11}5s^2$ configurations are within a relatively small interval below 274768 cm^{-1}. The first level with $5p$ electron, $4f^{12}5p\ (^3H)^4G_{11/2}$, lies substantially higher, at 387658 cm^{-1} which significantly affects the lifetimes of the lower states.

We also employed RMBPT method for simpler one-particle, $4f^{14}nl$, and particle-hole configurations of Ir ions to compare with HFR results.

The values for low-lying levels are presented in the paper, much more extensive set of results is given in the Supplemental Material [5].

II. LEVEL CROSSINGS AND $4f$ ELECTRONS IN HIGHLY-CHARGE IONS

Detailed investigation of level crossings relevant to the design of optical atomic clocks with highly-charged ions and search for α-variation has been carried out in [6]. Ir ions have been considered in [1]. Below, we discuss level crossings in ions similar to the ones studies in this work.

Correlation and relativistic effects for the $4f - nl$ and $5p - nl$ multipole transitions in Er-like tungsten were investigated in Ref. [7]. Wavelengths, transition rates, and line strengths were calculated for the multipole (E1, M1, E2, M2, and E3) transitions between the excited [Cd]$4f^{13}5p^6nl$, [Cd]$4f^{14}5p^5nl$ configurations and the ground [Cd]$4f^{14}5p^6$ state in Er-like W^{6+} ion ([Cd]=[Kr]$4d^{10}5s^2$) using the relativistic many-body perturbation theory, including the Breit interaction.

The binding energies of the $4f$, $5p$, and $5s$ orbitals in Er-like ions [7] calculated in Dirac-Fock approximation as function of nuclear charge Z are plotted in Fig. 1. For better presentation, we scaled the energies with a factor of $(Z-55)^2$. We find that the $4f$ orbitals are more tightly bound than the $5p$ and $5s$ orbitals at low stages of ionization, while the $5p$ and $5s$ orbitals are more tightly bound than the $4f$ orbitals for highly ionized cases. This leads to crossing of $4f$ and $5s$ and $5p$ levels for some Z leading to interesting cases of optical or near-optical transitions in selected highly-charged ions. Large cancellation in binding energy values near the crossing (near $Z = 74$ in the example of Fig. 1) make accurate calculations of transition energies and line strengths very difficult [7].

In Ref. [8], Safronova *et al.* reported results of *ab initio* calculation of excitation energies, oscillator strengths, transition probabilities, and lifetimes in Sm-like ions with nuclear charge Z ranging from 74 to 100. Sm has $Z = 62$. One of the unique atomic properties of the samarium isoelectronic sequence is that the ground state changes

nine times starting from the [Kr]$4d^{10}5s^25p^64f^66s^2\ ^1S_0$ level for neutral samarium, Sm I, and ending with the [Kr]$4d^{10}4f^{14}5s^2\ ^1S_0$ level for 12 times ionized tungsten, W^{12+} [9].

Contributions of the $4f$-core-excited states in determination of atomic properties in the promethium isoelectronic sequence with $Z = 74 - 92$ were discussed in Ref. [10]. Excitation energies, transition rates, and lifetimes in Pm-like tungsten were evaluated for a large number of states. The ground state for the Pm-like W^{13+}, Re^{14+}, Os^{15+}, and Ir^{16+} is $4f^{13}5s^2\ ^2F_{7/2}$. For the next Pm-like ion, Pt^{17+}, the $4f^{14}5s\ ^2S_{1/2}$ state becomes the ground state and continues to be the ground state for higher Z because of the $4f - 5s$ level crossing

III. ENERGY LEVELS

Our HFR calculations include the following set of configurations:

- Ir^{16+}: $4f^{14}5s$, $4f^{14}5p$, $4f^{13}5s^2$, $4f^{13}5p^2$, $4f^{13}5s5p$, $4f^{12}5s^25p$, and $4f^{12}5s5p^2$.
- Ir^{17+}: $4f^{14}$, $4f^{13}5s$, $4f^{13}5p$, $4f^{12}5s^2$, $4f^{12}5s5p$, and $4f^{12}5p^2$.
- Ir^{18+}: $4f^{13}$, $4f^{12}5s$, $4f^{12}5p$, $4f^{11}5s^2$, and $4f^{11}5s5p$.

In Table I, we list the limited number of excitation energies in three iridium ions of interest. The energies are given in 1000 cm^{-1}. The superscipts a and b in this and following tables are seniority numbers used to distinguish levels that have the same electronic configurations, intermediate and final terms. We note that the energy differences between the doublet $4f^{13}5s^2\ ^2F_J$ levels and the $4f^{14}5s\ ^2S_{1/2}$ levels in Pm-like Ir^{16+} are very small, and the excitation energy of the $4f^{14}5p\ ^2P_{1/2}$ is larger than the excitation energy of the $4f^{14}5s\ ^2S_{1/2}$ by a factor of 12. All other levels listed in the third column of Table I belong to the $4f^{13}5s5p$ and $4f^{12}5s^25p$ configurations. First two excited states have transition frequencies to the ground state in the optical range. The energy differences between the $4f^{13}5s\ ^3F_J$ (with $J = 4$ and 3) levels and the $4f^{14}\ ^1S_0$ level in Nd-like Ir^{17+} is 4000-5000 cm^{-1} according to COWAN code. However, the uncertainties in these small energy differences may be particularly large. The excitation energies of the two other $4f^{13}5s\ ^3F_2$ and $4f^{13}5s\ ^1F_3$ levels are larger than the excitation energy of the $4f^{13}5s\ ^3F_3$ level by a factor of 6-7 and the corresponding transition wavelengths to the ground state are in optical range. Almost all other levels listed in the column 6 of Table I belong to the $4f^{12}5s^2$ and $4f^{12}5s5p$ configurations. Only two levels belonging to the $4f^{13}5p$ configuration have sufficiently low excitation energies to be included in our list of Nd-like Ir^{17+} levels in Table I.

The ^2F ground state doublet splitting of the $4f^{13}5s^2$ and $4f^{13}$ configurations in Pm-like Ir^{16+} and Pr-like Ir^{18+} ions differs by only 2%. The transition from the next excited state of Ir^{+18} to the ground state is already in UV range. The first 25 low-lying levels of the Pr-like Ir^{18+} ion belong to the $4f^{12}5s$ configuration, while the other 22 levels belong to the $4f^{11}5s^2$ configuration.

IV. WAVELENGTHS, OSCILLATOR STRENGTHS, AND TRANSITION RATES

In Table II, we present selected set of our results for wavelengths (λ in Å), weighted oscillator strengths (gf), and weighted transition rates (gA_r in 1/s) for transitions between the $4f$-core-excited states. Only transition with the largest values of gA_r ($gA_r > 10^{12}$ s^{-1}) are given.

We find that the $4f^{12}5s^25p - 4f^{12}5s5p^2$ transitions have the largest values of gA_r for the Pm-like Ir^{16+}. This is expected since these arise from the one-electron electric-dipole $5s - 5p$ transitions. The same type of the transitions are the strongest for the other two ions; the $4f^{12}5s^2 - 4f^{12}5s5p$ and $4f^{12}5s5p - 4f^{12}5p^2$ transitions for the Nd-like Ir^{17+} ion and $4f^{11}5s^2 - 4f^{11}5s5p$ transitions in Pr-like Ir^{18+} ion, respectively. The transitions with the largest values of gA_r have wavelengths in the 187 - 200 Å range in Ir^{16+}, 187 - 214 Å range in Ir^{17+}, and 182 - 191 Å range in Ir^{18+}.

V. SYNTHETIC SPECTRA

Synthetic spectra for three Ir highly-charged ions are presented in Figs. 2, 3, and 4, respectively. We assume that spectral lines have the intensities proportional to the transition probabilities and are fitted with the Gaussian profile.

Synthetic spectra displayed in Figs. 2-4 are constructed from the following transitions:

- Ir^{16+}: $[4f^{14}5s + 4f^{13}5s5p + 4f^{12}5s5p^2] \leftrightarrow [4f^{14}5p + 4f^{13}5s^2 + 4f^{12}5s^25p]$,
- Ir^{17+}: $[4f^{14} + 4f^{13}5p + 4f^{12}5s^2] \leftrightarrow [4f^{13}5s + 4f^{12}5s5p]$,
- Ir^{17+}: $[\ 4f^{13} + 4f^{12}5p + 4f^{11}5s^2] \leftrightarrow [\ 4f^{12}5s + 4f^{11}5s5p]$.

Every spectrum on the left panel of the figure includes about 2000 transitions with the values of $gA_r > 10^{10}$ s^{-1}. The synthetic spectra on the right panel include lines with the largest gA_r values. For example, the spectrum of Ir^{16+} displayed on the left panel of Fig. 2 includes the spectral region 140Å - 360Å . In the right panel of Fig. 2, we limit this region to 180Å - 230Å by neglecting the part of spectra with small intensity with the A_r value less than 10 in units of $10^{10}s^{-1}$. The similar procedure was used for the other synthetic spectra.

Comparison of spectra at the right panels of of Figs. 2, 3, and 4 shows the similarities including the main

TABLE II: Wavelengths (λ in Å), weighted oscillator strengths (gf), weighted transition rates (gA_r in 1/s) for transitions in Pm-like Ir^{16+}, Nd-like Ir^{17+}, and Pr-like Ir^{18+} ions.

Conf.	Level	Conf.	Level	λ in Å	gf	gA_r in 1/s
$4f^{12}5s^25p - 4f^{12}5s5p^2$ transitions in Pm-like Ir^{16+} ion						
$4f^{12}5s^25p$	$(^1I)^2K_{15/2}$	$4f^{12}5s5p^2$	$(^1I)^2K^a_{15/2}$	187.3222	12.1796	2.315[12]
$4f^{12}5s^25p$	$(^3H)^4I_{15/2}$	$4f^{12}5s5p^2$	$(^3H)^4I^a_{15/2}$	188.4095	7.6206	1.432[12]
$4f^{12}5s^25p$	$(^3H)^4I_{13/2}$	$4f^{12}5s5p^2$	$(^3H)^4I^b_{13/2}$	189.4141	10.2303	1.902[12]
$4f^{12}5s^25p$	$(^1I)^2H_{11/2}$	$4f^{12}5s5p^2$	$(^1I)^2H^a_{11/2}$	190.2284	7.7758	1.433[12]
$4f^{12}5s^25p$	$(^1G)^2H_{11/2}$	$4f^{12}5s5p^2$	$(^3H)^2I^b_{11/2}$	190.2870	7.6461	1.408[12]
$4f^{12}5s^25p$	$(^1I)^2K_{13/2}$	$4f^{12}5s5p^2$	$(^1I)^2K^a_{13/2}$	190.5154	9.7403	1.790[12]
$4f^{12}5s^25p$	$(^1I)^2I_{13/2}$	$4f^{12}5s5p^2$	$(^1I)^2H^a_{11/2}$	191.9017	6.8966	1.249[12]
$4f^{12}5s^25p$	$(^1D)^2F_{7/2}$	$4f^{12}5s5p^2$	$(^1D)^2F^a_{7/2}$	192.6116	5.6848	1.022[12]
$4f^{12}5s^25p$	$(^3H)^4G_{11/2}$	$4f^{12}5s5p^2$	$(^3H)^4G^b_{11/2}$	192.9081	5.5967	1.003[12]
$4f^{12}5s^25p$	$(^3H)^4I_{11/2}$	$4f^{12}5s5p^2$	$(^3H)^2I^b_{11/2}$	193.3102	7.1596	1.278[12]
$4f^{12}5s^2 - 4f^{12}5s5p$ and $4f^{12}5s5p - 4f^{12}5p^2$ transitions in Nd-like Ir^{17+} ion						
$4f^{12}5s5p$	$(^1I)^3K_8$	$4f^{12}5p2$	$(^1I)^3K_8$	186.9139	5.5800	1.065[12]
$4f^{12}5s^2$	$(^1I)^1I_6$	$4f^{12}5s5p$	$(^1I)^1I_6$	187.4003	8.8646	1.684[12]
$4f^{12}5s^2$	$(^3H)^3H_6$	$4f^{12}5s5p$	$(^3H)^3H^b_6$	190.4460	7.6415	1.405[12]
$4f^{12}5s^2$	$(^3H)^3H_4$	$4f^{12}5s5p$	$(^3H)^3H^b_4$	191.2123	5.6115	1.024[12]
$4f^{12}5s^2$	$(^3H)^3H_5$	$4f^{12}5s5p$	$(^3H)^3I^b_6$	194.1681	7.6418	1.352[12]
$4f^{12}5s^2$	$(^3H)^3H_6$	$4f^{12}5s5p$	$(^3H)^3I^a_7$	194.6655	9.2353	1.625[12]
$4f^{12}5s^2$	$(^1I)^1I_6$	$4f^{12}5s5p$	$(^1I)^1K_7$	195.6155	8.9236	1.555[12]
$4f^{12}5s5p$	$(^1I)^1I_6$	$4f^{12}5p2$	$(^1I)^1I^b_6$	201.1890	7.8226	1.289[12]
$4f^{12}5s5p$	$(^1I)^1K_7$	$4f^{12}5p2$	$(^1I)^3K_8$	213.6590	6.9882	1.021[12]
$4f^{11}5s^2 - 4f^{11}5s5p$ transitions in Pr-like Ir^{18+} ion						
$4f^{11}5s^2$	$(^2F)^2F^1_{7/2}$	$4f^{11}5s5p$	$(^2F)^2F^1_{7/2}$	182.4907	5.6811	1.138[12]
$4f^{11}5s^2$	$(^2L)^2L_{15/2}$	$4f^{11}5s5p$	$(^2L)^2L^b_{15/2}$	184.2146	11.5687	2.274[12]
$4f^{11}5s^2$	$(^2L)^2L_{17/2}$	$4f^{11}5s5p$	$(^2L)^2L^b_{17/2}$	184.3734	8.2009	1.609[12]
$4f^{11}5s^2$	$(^2I)^2I_{13/2}$	$4f^{11}5s5p$	$(^2I)^2I^b_{13/2}$	186.7641	7.6961	1.472[12]
$4f^{11}5s^2$	$(^2G)^2G^2_{7/2}$	$4f^{11}5s5p$	$(^2G)^2H^2_{9/2}$	187.6959	5.6285	1.066[12]
$4f^{11}5s^2$	$(^4I)^4I_{15/2}$	$4f^{11}5s5p$	$(^4I)^4I^b_{15/2}$	187.7941	10.0169	1.894[12]
$4f^{11}5s^2$	$(^4I)^4I_{13/2}$	$4f^{11}5s5p$	$(^4I)^4I^b_{13/2}$	187.9089	7.4924	1.415[12]
$4f^{11}5s^2$	$(^2H)^2H^2_{9/2}$	$4f^{11}5s5p$	$(^2H)^2I^2_{11/2}$	188.0677	6.8954	1.300[12]
$4f^{11}5s^2$	$(^2H)^2H^1_{11/2}$	$4f^{11}5s5p$	$(^2I)^2K^b_{13/2}$	188.1826	6.6946	1.261[12]
$4f^{11}5s^2$	$(^4I)^4I_{11/2}$	$4f^{11}5s5p$	$(^4I)^4I^b_{11/2}$	188.3409	6.1020	1.147[12]
$4f^{11}5s^2$	$(^4G)^4G_{9/2}$	$4f^{11}5s5p$	$(^4I)^4K^b_{11/2}$	188.5680	5.3585	1.005[12]

peak, some strong lines separate from the main peak and the second wide peak of small intensity. All strong lines are listed in Table II and Supplemental Material [5].

We note that present synthetic spectra do not take into account the population of states, and are meant to illustrate the distribution on the strongest lines. In typical EBIT conditions many of the states are barely populated, making the spectra significantly less dense [11, 12].

VI. MULTIPOLE TRANSITIONS, BRANCHING RATIOS, AND LIFETIMES

Wavelengths, transition rates, energies of the lower and upper level, lifetimes, and branching ratios from M1 and E1 transitions in Nd-, Pm-, and Pr-like Ir ions are presented in Table III. In order to determine the lifetimes listed in the last columns of Table III, we sum over all possible radiative transitions. The value of branching ratios for the particular transition is determined as a ratio of the respective A_r values and the sum of all possible radiative transition rates that are used to determine the lifetimes. The number of contributing transitions increases significantly for higher levels. To save space, we only included the transitions that give the largest contributions to the lifetimes, and list additional transitions in the Supplemental Material [5].

We use atomic units (a.u.) to express all transition matrix elements throughout this section: the numerical values of the elementary charge, e, the reduced Planck constant, $\hbar = h/2\pi$, and the electron mass, m_e, are set equal to 1. The atomic unit for electric-dipole matrix element is ea_0, where a_0 is the Bohr radius.

The E1 and M1 transition probabilities A_r (s^{-1}) are obtained in terms of line strengths S (a.u.) and wave-

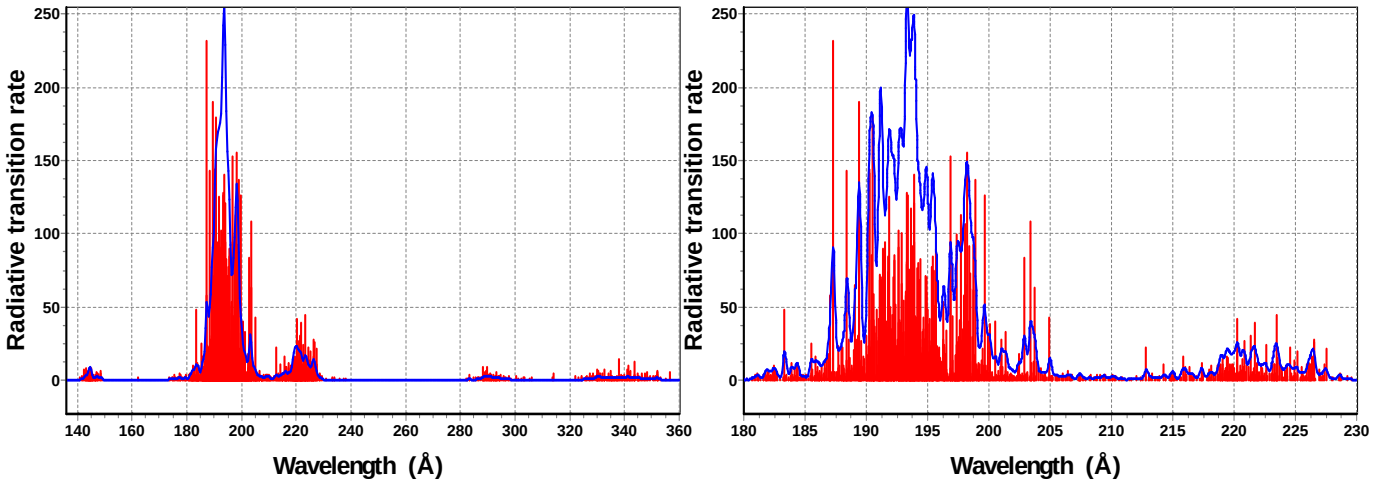

FIG. 2: Synthetic spectra (red) for the $[4f^{14}5s + 4f^{13}5s5p + 4f^{12}5s5p^2] \leftrightarrow [4f^{14}5p + 4f^{13}5s^2 + 4f^{12}5s^25p]$ transitions (red) in Pm-like Ir^{16+} as a function of wavelength. Promethium is a rare earth element with $Z = 61$. A resolving power, $R = E/\Delta E = 200$ and 600 (left and right) is assumed to produce a Gaussian profile (blue). The scale in the ordinate is in units of 10^{10} s^{-1}.

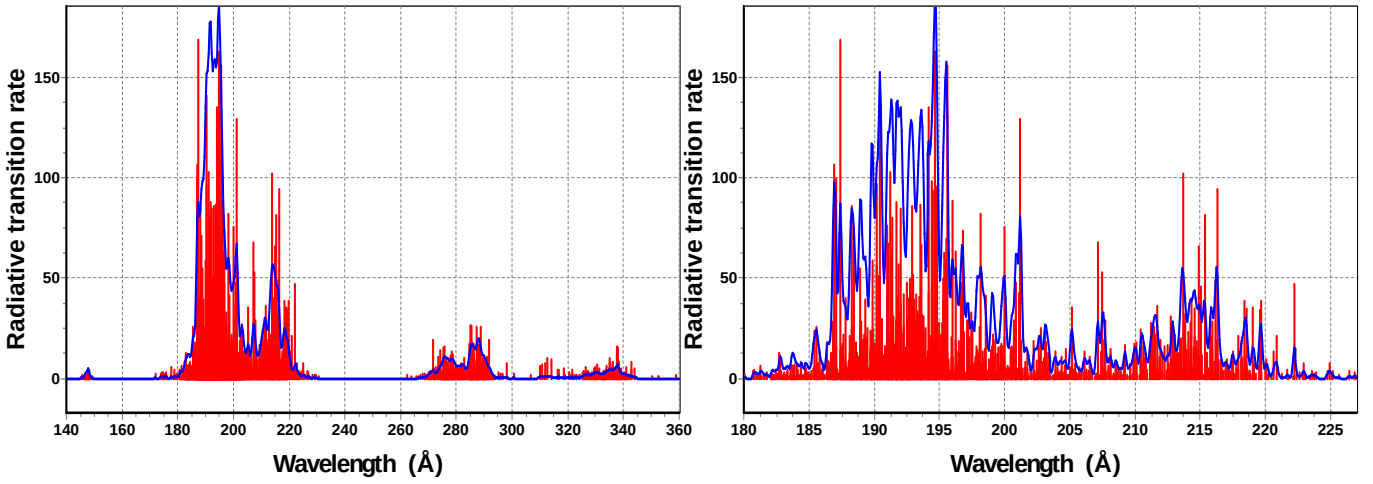

FIG. 3: Synthetic spectra (red) for the $[4f^{14} + 4f^{13}5p + 4f^{12}5s^2 + 4f^{12}5p^2] \leftrightarrow [4f^{13}5s + 4f^{12}5s5p]$ transitions (red) in Nd-like Ir^{17+} as a function of wavelength. Neodymium is a rare earth element with $Z = 60$. A resolving power, $R = E/\Delta E = 200$ and 800 (left and right) is assumed to produce a Gaussian profile (blue). The scale in the ordinate is in units of 10^{10} s^{-1}.

lengths λ (Å) as

$$A(E1) = 2.02613 \times 10^{18} \frac{S(E1)}{(2J+1)\lambda^3}, \quad (1)$$

$$A(M1) = 2.69735 \times 10^{13} \frac{S(M1)}{(2J+1)\lambda^3}. \quad (2)$$

The line strengths $S(E1)$ and $S(M1)$ are obtained as squares of the corresponding E1 and M1 matrix elements.

In Table III, we include results for 8 selected electric-dipole and magnetic-mulipole transitions that are the most important for the evaluation of the corresponding lifetimes in Pm-like Ir^{16+} ion. Results for 48 transitions contributing to the lifetimes of 32 lowest levels are listed in the Supplemental Material [5]. Transitions with small branching ratios are omitted from the table.

The second excited state, $4f^{14}5s\ ^2S_{1/2}$, is metastable with extremely long lifetime since the strongest possible decay channels are electric-octupole (E3) transition to the ground state, which is in optical range, and magnetic-quadrupole (M2) transition for the first excited level, $4f^{13}5s^2\ ^2F_{5/2}$. These transitions are too weak to be estimated with the COWAN code, so we described such cases in text but omit from the Table III. There is only one such level for Ir^{16+} and Ir^{16+} ions and two levels for

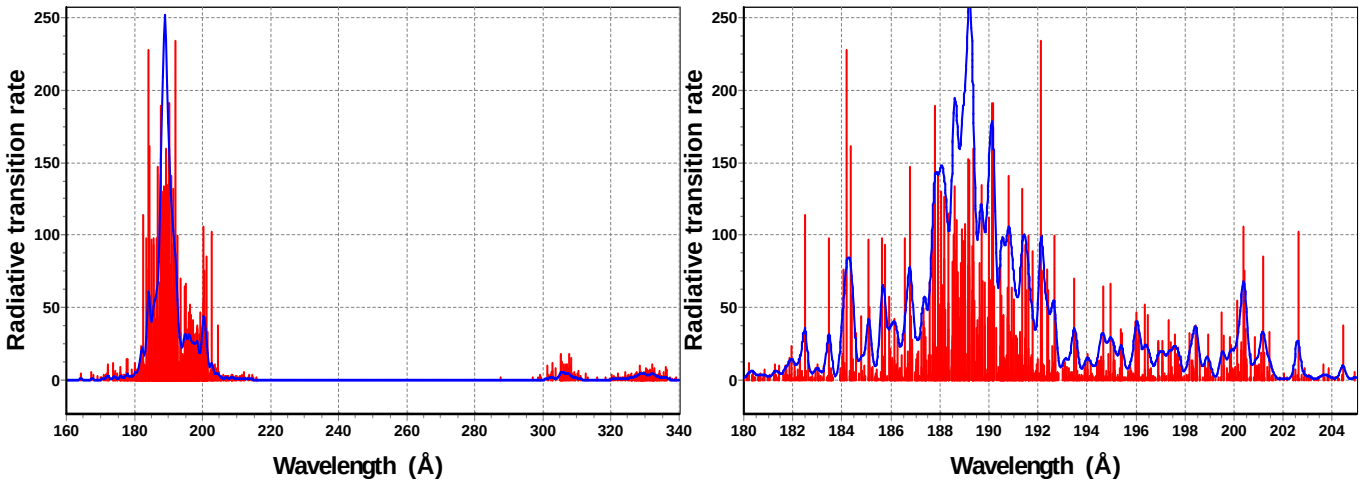

FIG. 4: Synthetic spectra (red) for the $[4f^{13} + 4f^{12}5p + 4f^{11}5s^2] \leftrightarrow [4f^{12}5s + 4f^{11}5s5p]$ transitions (red) in Pr-like Ir^{18+} as a function of wavelength. Praseodymium (Pr) is a rare earth element with $Z = 59$. A resolving power, $R = E/\Delta E = 200$ and 800 (left and right) is assumed to produce a Gaussian profile (blue). The scale in the ordinate is in units of 10^{10} s^{-1}.

Ir^{17+} ion.

The lifetime of the first excited $4f^{13}5s^2\ ^2F_{5/2}$ state is equal to 3.71 ms with A_r equal to 269 s^{-1}. The lifetime of the third excited state is very short, 7.8 ns due to E1 allowed $4f^{13}5s^2\ ^2F_{7/2} - 4f^{13}5s5p\ ^4D_{7/2}$ transition. The $4f^{12}5s^25p\ ^2I_{13/2}$ excited state is metastable with 4.65 s lifetime since the strongest transition is $4f^{12}5s^25p\ ^4G_{11/2}$–$4f^{12}5s^25p\ ^2I_{13/2}$ with small transition energy, 4298 cm^{-1}.

While some of the E1 transitions listed in Table III are strong allowed $5s - 5p$ transitions, a number of E1 transitions are very weak since these are forbidden transitions with non-zero amplitude due to configuration mixing. For example, the A_r value of the $4f^{13}5s^2\ ^2F_{7/2}$ - $4f^{13}5s5p\ ^4G_{9/2}$ transition is lager by nine orders of magnitude than $4f^{13}5s5p\ ^4D_{7/2}$ - $4f^{12}5s^25p\ ^4D_{7/2}$ transition. In the first case, we have one-electron E1-allowed $5s - 5p$ transition, while the second case is a strongly forbidden $4f - 5s$ transition. The non-zero value of the $4f^{13}5s5p\ ^4D_{7/2}$ - $4f^{12}5s^25p\ ^4D_{7/2}$ matrix element is due to mixing configurations.

In Table III, we include results for 10 selected electric-dipole and magnetic-mulipole transitions that are the most important for the evaluation of the corresponding Ir^{17+} lifetimes. Results for 33 transitions contributing to the lifetimes of 13 lowest levels are listed in the Supplemental Material [5]. We also evaluated electric-quadrupole transitions, however, their contributions to lifetimes of levels given in Table III is negligible. Four of the transitions listed in Table III are M1 transitions between the states inside of the $4f^{13}5s$ or $4f^{12}5s^2$ configurations. While the $4f^{13}5s - 4f^{12}5s^2$ transitions are E1-forbidden, their transition rates are non-zero due to mixing of the $4f^{13}5s$ and the $4f^{12}5s5p$ configurations. The lifetimes of most levels given in Table III are relatively long, since there are no allowed E1 transitions that may contribute to these lifetimes until the first level containing the $5p$ electron. The resulting lifetime of the $4f^{12}5s5p\ ^5G_6$ level is very short, 3.68 ns due to the $4f^{12}5s^2 - 4f^{12}5s5p$ E1 transitions.

Two Ir^{17+} levels, $4f^{14}\ ^1S_0$ and $4f^{12}5s^2\ ^3H_6$, are extremely long lived making then potential candidates for the atomic clock scheme implementation. There is only extremely weak electric-octupole transition to the $4f^{13}5s\ (^2F)^3F_3$ state contributing to $^1S_0$ lifetime. The $4f^{12}5s^2\ ^3H_6$ lifetime is determined by the two the E3 and one M2 channels: $4f^{13}5s\ ^3F_3$ - $4f^{12}5s^2\ ^3H_6$, $4f^{13}5s\ ^1F_3$ - $4f^{12}5s^2\ ^3H_6$, and $4f^{13}5s\ ^3F_4$ - $4f^{12}5s^2\ ^3H_6$.

In Table III, we include results for 10 selected electric-dipole and magnetic-multipole transitions that are most important for the evaluation of the corresponding lifetimes in Pr-like Ir^{18+} ion. Results for 51 transitions contributing to the lifetimes of 29 lowest levels are listed in the Supplemental Material [5]. Almost all transitions in Table III are magnetic-dipole transitions. Only last two lines include E1 forbidden transitions between $4f^{12}5s$ and $4f^{11}5s^2$ configurations. List of levels for the Pr-like Ir^{18+} ion in Table I covers the energy interval from the ground state up to 274768 cm^{-1}. The first level with $5p$ electron ($4f^{12}5p\ ^4G_{11/2}$ level) has energy equal to 387658 cm^{-1}. As a result, there are no electric-dipole allowed transitions in Table III.

The only extremely long-lived metastable level in Ir^{+18} ion is $4f^{12}5s\ ^4H_{13/2}$ third excited state with $E = 60142$ cm^{-1}. This state can only decay via very weak electric-octupole transition to the ground state, which is in UV range.

The next longest lifetime, 8100 s, is for the $4f^{12}5s\ ^2I_{11/2}$ level due to very small, 205 cm^{-1}, energy

TABLE III: Wavelengths (λ in Å), transition rates (A_r in s^{-1}), energies of the lower and upper level (cm^{-1}), lifetimes (τ), and branching ratios (Branch. ratio) for M1 and E1 transitions in Pm-like Ir^{16+}, Nd-like Ir^{17+}, and Pr-like Ir^{18+} ions.

Conf. Upper Level	Level	Conf. Lower level	Level		Energies in cm^{-1} Lower	Upper	λ Å	A_r 1/s	Branch. ratio	τ
Wavelengths, transition rates, lifetimes, and branching ratios from M1 and E1 transitions in Pm-like Ir^{16+} ion										
$4f^{13}5s^2$	$(^2F)^2F_{5/2}$	$4f^{13}5s^2$	$(^2F)^2F_{7/2}$	M1	0	25909	3860	2.69[+2]	1.00	3.71 ms
$4f^{13}5s5p$	$(^2F)^4D_{7/2}$	$4f^{13}5s^2$	$(^2F)^2F_{7/2}$	E1	0	267942	373	1.24[+8]	0.97	7.80 ns
$4f^{12}5s^25p$	$(^3H)^4G_{11/2}$	$4f^{13}5s^2$	$(^2F)^2F_{7/2}$	E2	0	276214	362	1.19[+2]	1.00	8.37 ms
$4f^{12}5s^25p$	$(^3H)^2I_{13/2}$	$4f^{12}5s^25p$	$(^3H)^4G_{11/2}$	M1	276214	280512	23271	2.15[-1]	1.00	4.65 s
$4f^{13}5s5p$	$(^2F)^4D_{7/2}$	$4f^{13}5s^2$	$(^2F)^2F_{7/2}$	E1	0	286286	349	3.54[+9]	0.98	0.278 ns
$4f^{12}5s^25p$	$(^3F)^4D_{7/2}$	$4f^{13}5s5p$	$(^2F)^4D_{7/2}$	E1	267942	285301	5761	2.27[+0]	0.94	0.415 s
		$4f^{13}5s^2$	$(^2F)^2F_{7/2}$	M1	0.000	285301	351	5.20[-2]	0.02	
		$4f^{13}5s^2$	$(^2F)^2F_{5/2}$	M1	25.909	285301	385	8.49[-2]	0.04	
$4f^{12}5s^25p$	$(^1G)^2H_{9/2}$	$4f^{13}5s5p$	$(^2F)^4D_{7/2}$	E1	267942	287909	5008	5.75[0]	0.92	0.161 s
		$4f^{13}5s^2$	$(^2F)^2F_{5/2}$	E2	25909	287909	382	1.80[-1]	0.03	
		$4f^{12}5s^25p$	$(^3H)^4G_{11/2}$	M1	276214	287909	23271	3.01[-1]	0.05	
$4f^{13}5s5p$	$(^2F)^4G_{9/2}$	$4f^{13}5s^2$	$(^2F)^2F_{7/2}$	E1	0	288623	346	4.69[+9]	1.00	0.213 ns
$4f^{13}5s5p$	$(^2F)^4F_{5/2}$	$4f^{13}5s^2$	$(^2F)^2F_{7/2}$	E1	0	289959	345	3.48[+9]	1.00	0.288 ns
$4f^{13}5s5p$	$(^2F)^4G_{5/2}$	$4f^{13}5s^2$	$(^2F)^2F_{7/2}$	E1	0	297128	337	1.66[+9]	0.83	0.499 ns
		$4f^{13}5s^2$	$(^2F)^2F_{5/2}$	E1	25909	297128	369	3.40[+8]	0.17	
Wavelengths, transition rates, lifetimes, and branching ratios from M1 and E1 transitions in Nd-like Ir^{17+} ion										
$4f^{13}5s$	$(^2F)^3F_3$	$4f^{13}5s$	$(^2F)^3F_4$	M1	0	4236	23610	1.18[+0]	1.00	849 ms
$4f^{13}5s$	$(^2F)^3F_2$	$4f^{13}5s$	$(^2F)^3F_3$	M1	4236	26174	4558	2.26[+2]	1.00	4.42 ms
$4f^{13}5s$	$(^2F)^1F_3$	$4f^{13}5s$	$(^2F)^3F_4$	M1	0	30606	3267	3.05[+2]	1.00	3.27 ms
$4f^{12}5s^2$	$(^3F)^3F_4$	$4f^{13}5s$	$(^2F)^3F_3$	E1	4236	42199	2634	6.51[+1]	0.97	14.9 ms
		$4f^{13}5s$	$(^2F)^1F_3$	E1	30606	42199	8626	1.79[+0]	0.03	
$4f^{12}5s^2$	$(^3H)^3H_5$	$4f^{12}5s^2$	$(^3H)^3H_6$	M1	33855	58261	4097	3.80[+2]	1.00	2.63 ms
$4f^{12}5s^2$	$(^3F)^3F_2$	$4f^{13}5s$	$(^2F)^3F_3$	E1	4236	63696	1682	2.55[+2]	0.71	2.79 ms
		$4f^{13}5s$	$(^2F)^1F_3$	E1	30606	63696	3022	1.04[+2]	0.29	
$4f^{12}5s5p$	$(^3H)^5G_6$	$4f^{12}5s^2$	$(^3H)^3H_6$	E1	33856	312026	359	2.65[+8]	0.97	3.68 ns
		$4f^{12}5s^2$	$(^3H)^3H_5$	E1	58261	312026	394	6.72[+6]	0.03	
Wavelengths, transition rates, lifetimes, and branching ratios from M1 and E1 transitions in Pr-like Ir^{18+} ion										
$4f^{13}$	$(^2F)^2F_{5/2}$	$4f^{13}$	$(^2F)^2F_{7/2}$	M1	0	26442	3782	2.86[+2]	1.00	3.49 ms
$4f^{12}5s$	$(^3H)^4H_{11/2}$	$4f^{12}5s$	$(^3H)^4H_{13/2}$	M1	60142	67687	13254	8.46[+0]	1.00	118 ms
$4f^{12}5s$	$(^3F)^4F_{9/2}$	$4f^{13}$	$(^2F)^2F_{7/2}$	E1	0	70096	1427	5.92[+2]	1.00	0.169 ms
$4f^{12}5s$	$(^1G)^2G_{7/2}$	$4f^{12}5s$	$(^3F)^4F_{9/2}$	M1	70096	74664	21892	1.54[+0]	1.00	650 ms
$4f^{12}5s$	$(^3H)^4H_{9/2}$	$4f^{12}5s$	$(^3H)^4H_{11/2}$	M1	67687	87749	4985	2.81[+2]	1.00	3.55 ms
$4f^{12}5s$	$(^3H)^2H_{11/2}$	$4f^{12}5s$	$(^3H)^4H_{13/2}$	M1	60142	89858	3365	4.30[+2]	1.00	2.33 ms
$4f^{12}5s$	$(^3F)^4F_{5/2}$	$4f^{12}5s$	$(^1G)^2G_{7/2}$	M1	74664	92939	5472	4.23[+1]	1.00	23.7 ms
$4f^{12}5s$	$(^3F)^4F_{7/2}$	$4f^{12}5s$	$(^3F)^4F_{9/2}$	M1	70096	94507	4096	6.23[+1]	0.36	5.86 ms
		$4f^{12}5s$	$(^1G)^2G_{7/2}$	M1	74664	94507	5039	1.01[+2]	0.59	
$4f^{12}5s$	$(^1G)^2G_{9/2}$	$4f^{12}5s$	$(^3F)^4F_{9/2}$	M1	70096	98485	3522	1.67[+2]	0.98	5.88 ms

difference in the $4f^{12}5s\ ^2I_{13/2} - 4f^{12}5s\ ^2I_{11/2}$ transition. The $4f^{11}5s^2\ ^2I_{13/2}$ level has short lifetime due to contribution of two E1 transitions via level mixing with branching ratios equal to 62% and 38%.

Dominant contribution to the $4f^{12}5s^4F_{9/2}$ lifetime is from E1-forbidden transition to the $4f^{13}\ ^2F_{7/2}$ state which is non-zero due to the 5% mixing between $4f^{13}$ and $4f^{12}5p$ configurations.

We did not find any theoretical or experimental results to compare with our A_r and τ values for the low-lying states listed in Table III.

VII. COMPARISONS, UNCERTAINTY ESTIMATES, AND CONCLUSION

In Table IV, we compare energies in Nd-like Ir^{17+} ion calculated using the COWAN and RMBPT codes. Details of the RMBPT code for the hole-particle systems

TABLE IV: Energies (in cm^{-1}) in Nd-like Ir^{17+} ions given relative to the $4f^{13}5s\ ^3F_4$ ground states. Comparison of the results calculated by the COWAN and RMBPT codes. The difference is given in percent in the last column.

Conf.	Level	Energy		Level		DIFF.
LSJ	designations	$E^{\rm COWAN}$	$E^{\rm RMBPT}$	jj	designations	J	%
$4f^{13}5s$	$(^2F)^3F_4$	0	0	$4f_{7/2}5s_{1/2}$		4	
$4f^{13}5s$	$(^2F)^3F_3$	4236	4129	$4f_{5/2}5s_{1/2}$		3	2.5
$4f^{14}$	$(^1S)^1S_0$	5091	7055	$4f^{14}$		0	-38.5
$4f^{13}5s$	$(^2F)^3F_2$	26174	25447	$4f_{7/2}5s_{1/2}$		3	2.8
$4f^{13}5s$	$(^2F)^1F_3$	30606	30374	$4f_{5/2}5s_{1/2}$		4	0.8
$4f^{13}5p$	$(^2F)^3D_3$	319802	316065	$4f_{7/2}5p_{1/2}$		3	1.2
$4f^{13}5p$	$(^2F)^3G_4$	322623	319341	$4f_{7/2}5p_{1/2}$		4	1.0
$4f^{13}5p$	$(^2F)^3G_3$	346618	341890	$4f_{5/2}5p_{1/2}$		3	1.4
$4f^{13}5p$	$(^2F)^3F_2$	352344	348344	$4f_{5/2}5p_{1/2}$		2	1.1
$4f^{13}5p$	$(^2F)^3G_5$	482729	478806	$4f_{7/2}5p_{3/2}$		5	0.8
$4f^{13}5p$	$(^2F)^3D_2$	485701	481145	$4f_{7/2}5p_{3/2}$		2	0.9
$4f^{13}5p$	$(^2F)^1F_3$	491623	488430	$4f_{7/2}5p_{3/2}$		3	0.6
$4f^{13}5p$	$(^2F)^3F_4$	497788	494305	$4f_{7/2}5p_{3/2}$		4	0.7
$4f^{13}5p$	$(^2F)^3D_1$	502142	497907	$4f_{5/2}5p_{3/2}$		1	0.8
$4f^{13}5p$	$(^2F)^3G_4$	512504	507690	$4f_{5/2}5p_{3/2}$		4	0.9
$4f^{13}5p$	$(^2F)^3F_2$	519370	516116	$4f_{5/2}5p_{3/2}$		2	0.6
$4f^{13}5p$	$(^2F)^3F_3$	523054	518658	$4f_{5/2}5p_{3/2}$		3	0.8

TABLE V: Wavelengths (λ in Å), weighted oscillator strengths (gf), weighted transition rates (gA_r in 1/s) for the $4f^{14}5s - 4f^{14}5p_j$ transitions in Pm-like Ir^{16+}. Comparison of the results evaluated using the first-order RMBPT1, second-order RMBPT2, and the COWAN codes. Numbers in brackets represent powers of 10

	RMBPT1	RMBPT2	COWAN
	$4f^{14}5s - 4f^{14}5p_{1/2}$ transition		
ΔE in cm^{-1}	312299	313974	309407
λ in Å	320.31	318.50	323.20
gf	0.5249	0.3809	0.3308
gA_r in 1/s	3.413[10]	2.522[10]	2.112[10]
	$4f^{14}5s - 4f^{14}5p_{3/2}$ transition		
ΔE in cm^{-1}	469050	472710	469871
λ in Å	213.20	211.55	212.82
gf	1.6045	1.1754	1.4855
gA_r in 1/s	2.355[11]	1.752[11]	2.187[11]

were presented by Safronova et. al. [13]. We use a complete set of Dirac-Fock (DF) wave functions on a nonlinear grid generated using B-splines [14] constrained to a spherical cavity. The basis set consists of 50 splines of order 9 for each value of the relativistic angular quantum number κ. The starting point for the RMBPT code is the *frozen core* DF approximation. We use second-order RMBPT to determine energies of the $4f^{13}5s$ states relatively to the $4f^{14}$ state in Nd-like Ir^{17+} ion.

The jj designation ($4f_{7/2}5s_{1/2}$ for example) listed in Table IV means that we consider the system with $4f_{7/2}$ hole in $4f^{14}$ core and the $5s_{1/2}$ particle. The LS designation are given in columns "1" and "2" of Table IV. The results with the same configuration and J are compared. The difference of RMBPT and COWAN data given in the last column of Table IV is less than 1% for most levels. The difference exceeds 3% only for $4f^{14}$ level. This is the only level in the table that has a different number of $4f$ electrons in comparison with the ground state. The correlation correction is very large for the $4f$ state leading to this difference. For example, the calculation of the $4f_{7/2}5s_{1/2}$ $J = 4$ ground state energy gives 5447 cm^{-1} in lowest order DF approximation, while the second order value is almost five times larger, -23997 cm^{-1}. Adding the 4577 cm^{-1} QED and 6888 cm^{-1} Breit corrections gives -7055 cm^{-1} relative to the frozen-core $4f^{14}$ level.

In Table V, we compare wavelengths, weighted oscillator strengths, and weighted transition rates for the $4f^{14}5s - 4f^{14}5p$ transitions in Pm-like Ir^{16+} evaluated using the first-order RMBPT1, second-order RMBPT2 [13], and the COWAN codes. COWAN code energy values are in somewhat better agreement with the first-order RMBPT results. The difference of RMBPT and COWAN code energies and wavelength is small, 0.18 % - 1.5 %, for wavelengths and energies of the $4f^{14}5s - 4f^{14}5p$.

The differences are larger, 7 % - 27 %, for the oscillator strength and transition rates. We find large effects of the second order corrections for these properties leading to larger differences in the results. In summary, the second-order correlation corrections are very important for accurate determination of the oscillator strengths and transition rates.

Energies (in cm^{-1}) in Nd-like Ir^{17+} ion relative to the $4f^{13}5s\ ^3F_4$ ground state obtained by the COWAN code are compared with results from Ref. [1] and [3] in Table VI. Results in [1] were obtained using configuration-interaction (CI) approach. Results in [3] were obtained using multireference Fock space coupled cluster (FSCC) method and configuration-interaction-Dirac-Fock-Sturmian (CIDFS) method. COWAN results were also presented in [3]. The largest difference (12%) between the COWAN and CI [1] results is for the first excited state. For other levels, the difference is about 3-4%. The largest difference (94%) between results in Ref. [3], evaluated by FSCC and CIDFS methods are for the $4f^{14}\ ^1S_0$ level. For other levels, the difference is about 5-9%.

Comparison of the present results with theoretical [1, 3] and experimental [3] transition energies (in cm^{-1}) for M1 transitions in Nd-like Ir^{17+} ion are given in Table VII. In [3], improved accuracy measurements were performed for the Ir^{17+} transitions by repeating a calibration-measurement-calibration cycle five times at one grating position. Each cycle takes 15-30 min. The transition energy was determined by averaging the line centroids in typically 30 of such acquired spectra. Results are given for the M1 transitions between the states of the $4f^{13}5s$ and $4f^{12}5s^2$ configurations. The differences between the experimental results and theoretical values obtained by the COWAN code, CI [1], FSCC and CIDFS [3] are given

TABLE VI: Comparison of the energies (in cm^{-1}) in Nd-like Ir^{17+} ion given relative to the $4f^{13}5s\ ^3F_4$ ground state obtained in different approximations [1, 3].

Conf.	Level	Energies in cm^{-1}		Diff.	Energies in cm^{-1}		Diff.
		COWAN	CI [1]	%	FSCC [3]	CIDFS [3]	%
$4f^{13}5s$	$(^2F)^3F_4$	0	0				
$4f^{13}5s$	$(^2F)^3F_3$	4236	4838	12%	4662	4872	4%
$4f^{13}5s$	$(^2F)^3F_2$	26174	26272	0%	25156	25044	0%
$4f^{13}5s$	$(^2F)^1F_3$	30606	31492	3%	30197	30552	1%
$4f^{14}$	$(^1S)^1S_0$	5091	5055	-1%	13599	7025	-94%
$4f^{12}5s^2$	$(^3H)^3H_6$	33856	35285	4%	24221	29367	18%
$4f^{12}5s^2$	$(^3F)^3F_4$	42199	45214	7%	33545	38295	12%
$4f^{12}5s^2$	$(^3H)^3H_5$	58261	59727	2%	47683	52668	9%
$4f^{12}5s^2$	$(^3F)^3F_2$	63696	68538	7%	55007	60322	9%
$4f^{12}5s^2$	$(^3H)^1G_4$	66296	68885	4%	56217	60943	8%
$4f^{12}5s^2$	$(^3F)^3F_3$	68886	71917	4%	58806	63847	8%
$4f^{12}5s^2$	$(^3H)^3H_4$	89455	92224	3%	78534	82954	5%
$4f^{12}5s^2$	$(^3P)^1D_2$	91765	98067	6%	82422	88261	7%
$4f^{12}5s^2$	$(^1I)^1I_6$	101537	110065	8%	93867	101844	8%
$4f^{12}5s^2$	$(^3P)^3P_0$	101073	110717	9%	94012	99617	6%
$4f^{12}5s^2$	$(^3P)^3P_1$	107843	116372	7%	99416	105989	6%
$4f^{12}5s^2$	$(^1D)^3P_2$	117322			107489	113272	5%
$4f^{12}5s^2$	$(^1S)^1S_0$	178055			174893	185757	6%

TABLE VII: Comparison of the present results with theoretical [1, 3] and experimental [3] transition energies (in cm^{-1}) for M1 transitions in Nd-like Ir^{17+} ion. Differences between experimental and theoretical results are given in per cent for all theoretical values.

Conf.	Transition	Energy Expt. [3]	Energy COWAN	Diff. %	Energy CI [1]	Diff. %	Energy FSCC [3]	Diff. %	Energy CIDFS [3]	Diff. %
$4f^{13}5s$	$^3F_2 - {}^3F_3$	20710.83	21938	-6%	21434	-3%	20494	1%	20172	3%
$4f^{12}5s^2$	$^3H_4 - {}^1G_4$	22430.03	23159	-3%	23339	-4%	22317	1%	22011	2%
$4f^{12}5s^2$	$^1G_4 - {}^3F_4$	22948.54	24097	-5%	23671	-3%	22672	1%	22648	1%
$4f^{12}5s^2$	$^1D_2 - {}^3F_3$	23162.84	22879	1%	26150	-13%	23616	-2%	24414	-5%
$4f^{12}5s^2$	$^3H_5 - {}^3H_6$	23639.87	24405	-3%	24442	-3%	23462	1%	23301	1%
$4f^{12}5s^2$	$^3F_3 - {}^3F_4$	25514.56	26687	-5%	26703	-5%	25261	1%	25552	0%
$4f^{12}5s^2$	$^1D_2 - {}^3F_2$	27387.06	28069	-2%	29529	-8%	27415	0%	27939	-2%
$4f^{13}5s$	$^1F_3 - {}^3F_4$	30358.45	30606	-1%	31492	-4%	30197	1%	30552	-1%
$4f^{12}5s^2$	$^3H_4 - {}^3H_5$	30797.17	31194	-1%	32497	-6%	30851	0%	30286	2%

in percent. The largest difference between the experimental values [3] and the COWAN code results is 6%, while the difference is twice as large for CI values [1]. The differences between the FSCC [3] and CIDFS [3] results and experiment [3] are 0-2% and 0-5%, respectively.

One of the main challenges in implementation of the clock schemes with highly-charged ions will be experimental identification of the very narrow line clock transitions as well as other transitions than may be used for cooling. Spectra identification is the first step towards this goal. We find that Cowan code results are in very good agreement with experiment, 1-6% for M1 transition energies. Cowan code results are in better agreement with experiment for the measured transitions than the CI calculations and in general give accuracy similar to the CIDFS. However, the experimental data for the even-to-odd transition energies are not yet available and lack of other benchmarks does not allow to evaluate the accuracy for these quantities even for the most elaborate coupled-cluster FSCC method. When such measurements will become available, the accuracy of the Cowan code for the Ir^{17+} clock transition could be established, both yielding important benchmarks for other highly-charged ion system and allowing to further improve Ir^{17+} predictions for yet unmeasured transitions.

In summary, we carried out a systematic study of excitation energies, wavelengths, oscillator strengths, and transition rates in Ir^{16+}, Ir^{17+}, and Ir^{18+} ions. Synthetic spectra are constructed for all three ions, with the strongest line regions presented in more detailed on a separate panel. Metastable states and importance of the M1 transitions for the determination of the lifetimes are discussed. Comparison of the energy values with other theoretical predictions is given. Transition wavelengths

are compared with the experiment [3] and other theory. We did not find any other theoretical results of oscillator strength and transitions rates in the ions considered in the present study. We believe that our predictions will be useful for planning and analyzing future experiments with highly-charged ions.

Acknowledgements

We thank H. Bekker, A. Windberger, and J. R. Crespo López-Urrutia for discussions and comments on the paper. M. S. S. thanks the School of Physics at UNSW, Sydney, Australia and MPIK, Heidelberg, Germany for hospitality and acknowledges support from the Gordon Godfrey Fellowship program, UNSW. This work was supported in part by U. S. NSF Grant No. PHY-1404156 and the Australian Research Council.

[1] J. C. Berengut, V. A. Dzuba, V. V. Flambaum, and A. Ong, Physical Review Letters **106**, 210802 (2011), 1103.2823.
[2] L. Schmöger, O. O. Versolato, M. Schwarz, M. Kohnen, A. Windberger, B. Piest, S. Feuchtenbeiner, J. Pedregosa-Gutierrez, T. Leopold, P. Micke, et al., Science **347**, 1233 (2015).
[3] A. Windberger, J. R. Crespo López-Urrutia, H. Bekker, N. S. Oreshkina, J. C. Berengut, V. Bock, A. Borschevsky, V. A. Dzuba, E. Eliav, Z. Harman, et al., Phys. Rev. Lett. **114**, 150801 (2015).
[4] H. Bekker, O. O. Versolato, A. Windberger, N. S. Oreshkina, R. Schupp, T. M. Baumann, Z. Harman, C. H. Keitel, P. O. Schmidt, J. Ullrich and J. R. Crespo López-Urrutia, J. Phys. B, in press (2015).
[5] See Supplemental Material at [URL] for tabulation of excitation energies, wavelengths, transition rates, energies of the lower and upper level, lifetimes, and branching ratios from M1 and E1 transitions in Nd-, Pm-, and Pr-like Ir ions.
[6] J. C. Berengut, V. A. Dzuba, V. V. Flambaum, and A. Ong, Phys. Rev. A **86**, 022517 (2012).
[7] U. I. Safronova and A. S. Safronova, Phys. Rev. A **84**, 012511 (2011).
[8] U. I. Safronova, A. S. Safronova, and P. Beiersdorfer, Phys. Rev. A **87**, 032508 (2013).
[9] A. Kramida, Yu. Ralchenko, J. Reader, and the NIST ASD Team (2012). NIST Atomic Spectra Database (version 5.0). Available at http://physics.nist.gov/asd [2012, November 12]. National Institute of Standards and Technology, Gaithersburg, MD.
[10] U. I. Safronova, A. S. Safronova, and P. Beiersdorfer, Phys. Rev. A **88**, 032512 (2013).
[11] Y. Kobayash, D. Kato, H. A. Sakaue, I. Murakami and N. Nakamura, Phys. Rev. A 89, 010501 (2014).
[12] H. Bekker, private communication.
[13] U. I. Safronova, , W. R. Johnson, and J. R. Albritton, Phys. Rev. A **62**, 052505 (2000).
[14] W. R. Johnson, S. A. Blundell, and J. Sapirstein, Phys. Rev. A **37**, 307 (1988).